

Thermodynamic Study of Hg(II) Ion Adsorption onto Nano Hydroxyapatite from Aqueous Solution

S. Ghasemlou^{1,*}, H. Aghaie² and M. Monajjemi²

¹Ph. D. Student, Department of Chemistry, Tehran Science and Research Branch, Islamic Azad University, Tehran, Iran

²Department of Chemistry, Tehran Science and Research Branch, Islamic Azad University, Tehran, Iran

Received February 2014; Accepted February 2014

ABSTRACT

Hydroxyapatite nanocrystals were synthesized by sol-gel combustion method for the sorption of Hg(II) ions from aqueous solutions. The effects of varying parameters such as pH, temperature, initial metal concentration, and contact time on the adsorption process were examined. Adsorption equilibrium was established in 360 minutes and the maximum adsorption of Hg(II) on the hydroxyapatite was observed to occur at pH 7.0. The adsorption data correlated with Freundlich and Langmuir isotherms. The Langmuir isotherm showed a better fit to the equilibrium data. The adsorption thermodynamic parameters (ΔG^0 , ΔH^0 , and ΔS^0) were calculated which showed an endothermic adsorption process. The equilibrium parameter (R_L) indicated that hydroxyapatite nanocrystals are useful for Hg(II) removal from aqueous solutions.

Keywords: Adsorption; Nano Hydroxyapatite; Hg(II) Removal; Isotherm; Thermodynamics

INTRODUCTION

Due to heavy metals toxicity and non-biodegradable nature, the introduction of heavy metals in water has been an increasingly serious environmental and public health concern. A number of technologies have been developed to remove toxic heavy metals from wastewater. Furthermore, automotive, electronics, metal finishing and oil sands industries form a large economic sector in

Iran. These industries generate a large quantity of wastewater containing heavy metals such as Pb^{2+} , Cd^{2+} , Zn^{2+} , Ni^{2+} and the like. Typically, the wastewater from the metal finishing industry (e-coating process) contains 20 ppm each of Zn^{2+} . On the other hand, the maximum allowable discharge concentration of Zn^{2+} and Ni^{2+} is 2 ppm [1]. Various methods have been used to remove heavy metals from wastewater,

*Corresponding author: ghasemlou@gmail.com

including: reduction and precipitation [2], coagulation and flotation [3], adsorption [4, 5], ion exchange, membrane technologies and electrolysis [6]. Generally, they are expensive or ineffective, especially when the metal concentration is higher than 100 ppm [7, 8]. Hydroxyapatite is an ideal material for long-term containment of contaminants because of its high sorption capacity for actinides and heavy metals, low water solubility, high stability under reducing and oxidizing conditions, availability, and low cost [9]. It was conducted in stabilization of a wide variety of metals by many investigators [10-15]. They reported the sorption to take place through ionic exchange reaction, surface complexation with phosphate, calcium and hydroxyl groups and/or co-precipitation of new partially soluble phases.

Calcium hydroxyapatite (CaHAp), $\text{Ca}_{10}(\text{PO}_4)_6(\text{OH})_2$, is used for the removal of heavy metals from contaminated soils, wastewater and fly ashes [16-22]. Calcium hydroxyapatite (CaHAp) is a main component of animal hard tissues and has been of interest in industry and medical fields. Its synthetic particles have many applications in bioceramics and chromatographic adsorbents [23]. These properties relate to various surface characteristics of HAp, e.g., surface functional groups, acidity and basicity, surface charge, hydrophilicity, and porosity. It has been found that HAp surface possesses 2.6 groups nm^{-2} of P-OH groups acting as sorption sites [24]. The sorption properties of HAp are of great importance for both environmental processes and industrial purposes.

The objective of this study was to explore the possible use of nano-crystalline hydroxyapatite as an alternative adsorbent material for the removing of Hg^{+2} ions from aqueous solutions. The Langmuir and Freundlich models were applied to fit the

equilibrium isotherm. The dynamic behavior of the adsorption was investigated on the effect of pH, temperature, initial metal concentration, and contact time. The thermodynamic parameters were also evaluated from the adsorption measurements.

EXPERIMENTAL

Materials and instrumental

The chemical reagents used included fumed $\text{Ca}(\text{NO}_3)_2 \cdot 4\text{H}_2\text{O}$ (Merck), $\text{C}_6\text{H}_7\text{O}_8$ (Merck), $(\text{NH}_4)_2\text{HPO}_4$ (Merck) and deionized water. A stock solution (1000 mg/L) of Hg(II) was prepared by dissolving appropriate amounts of HgCl (Merk) in double-distilled water. Phosphoric acid and sodium dihydrogen phosphate buffers, as well as 0.1 M HCl and 0.1 M NaOH were used to adjust pH of the solution in the range of 4.0–8.0. All chemicals were of analytical grade and were used without purifications. A scanning electron microscope (HITACHI SU660 SEM) was applied to characterize the hydroxyapatite nanocrystals. Also, an X-ray diffraction (XRD) analysis was performed with Siemens diffractometer with Cu K_α lamp in radiation ($\lambda=0.154$ nm) within the spectral range of 3–60° and the angle 2θ . The concentrations of mercury ions were measured by an atomic absorption spectrometer (VARIAN, AA240) equipped with air-acetylene flame. The operating parameters were: lamp current, 4.0 mA; slit width, 0.5 nm; wavelength, 253.7 nm. A PP775 portable pH meter and Eppendorf 5810 centrifuge were used for all pH measurements and centrifugations.

Preparation of nano hydroxyapatite

Hydroxyapatite compounds were prepared by sol-gel combustion method using $\text{Ca}(\text{NO}_3)_2 \cdot 4\text{H}_2\text{O}$ (9.8592 g), $(\text{NH}_4)_2\text{HPO}_4$ (3.3018 g) and citric acid (8.0212 g) as combustion agent as starting materials. At

first the precursors and a suitable fuel –as a reducing agent–were dissolved to specific molar ratios in 52/5ml of deionized water and a clear solution was obtained. Hydrolysis reaction was carried out in a thermostatic bath (80°C) for 3-4 hours. After gradual evaporation of water in the solution, a white thick gel was obtained that was transferred to the oven for calcination at 700°C (optimal temperature for maximal purity of hydroxyapatite nanoparticles and impurity decrease of β TCP (CaO and CaCO₃) and 950°C (maximal impurity) in 9 hours after being dried at 140°C and grinding the brown-black powder resulting from the combustion. During the combustion, such gases as CO₂ and NH₃ were released. At the end of the phase, a white compound was obtained from comprised hydroxyapatite nanoparticles.

Adsorption method

An adsorption experiment involved adding 0.05 g of nano hydroxyapatite to 10 ml of Hg(II) solution with initial concentration of 200 mg/L at pH 8. The suspension was mixed on a thermo-stated shaker bath operating at 30 °C and 150 rpm for duration of 360 minutes. The mixture was centrifuged at 5000 rpm for 10 minutes to separate the solid adsorbents from the solution. The final concentration of the metal ion was determined by flame atomic absorption spectroscopy (AAS). The effects of pH, temperature, initial concentration of Hg²⁺ ion, and contact time between adsorbates and adsorbent were investigated. All experiments were performed at least three times and average values of the results are given here. The amount of ions adsorbed per unit mass of adsorbent, q_e (mg/g) is evaluated using the following expression:

$$q_e = \frac{v(C_0 - C_e)}{w} \quad (1)$$

Where C_0 is the initial concentration and C_e is the equilibrium concentration, mg/L and v (L) is the volume of Hg(II) solution, and w (g) is the weight of adsorbent, namely nano hydroxyapatite.

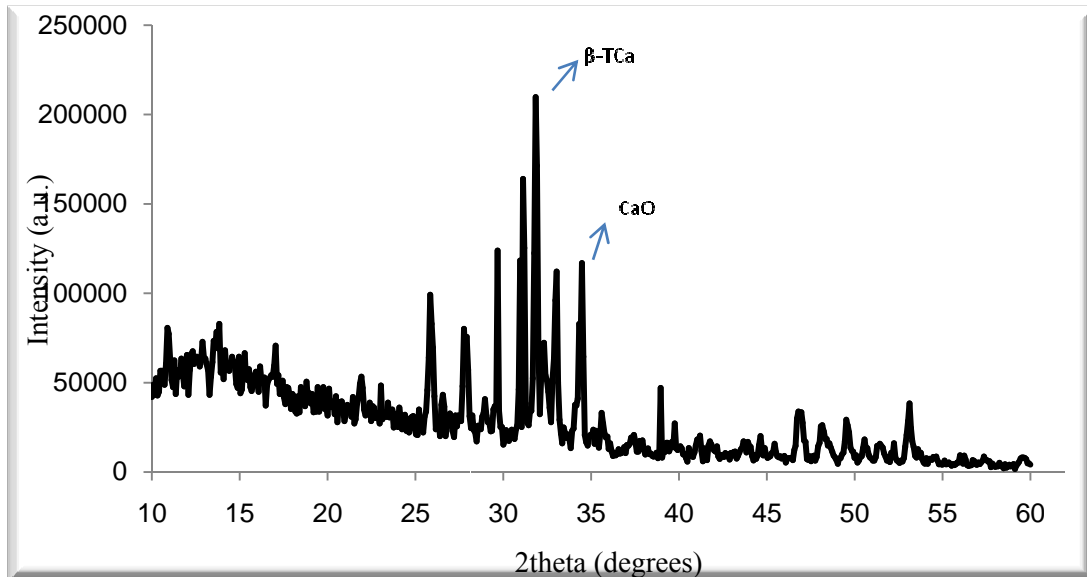
RESULTS AND DISCUSSION

The principal method for determining the degree of crystallinity of the crystalline samples is X-ray diffraction. The phase transition during heat treatment and crystallite size evolutions were carried out by X-ray diffraction analysis using a Siemens diffractometer with Cu K α lamp in radiation ($\lambda=0.154$ nm) within the spectral range of 3-60° and the angle 2θ . The main peak of hydroxyapatite which is around 30 to 35 degrees can be used as an indicator to determine the degree of crystallinity. The results of X-ray diffraction test on samples collected at 700°C (optimal temperature) and 950°C in Fig. 1 do not match thank to the severity of impurities, suggesting that the more temperature, the more impurity and crystallinity. The sample heated at 950°C showed a high degree of CaO and β – TCP impurity comparing with the optimal temperature (700°C) and showed that with increasing temperature from 700 to 950°C, the hydroxyapatite lines become thinner and the intensity of peaks increases gradually, suggesting more crystallinity of the samples at this temperature. In addition, it was observed that the more temperature, the more severe peaks of CaO and β – TCP impurity.

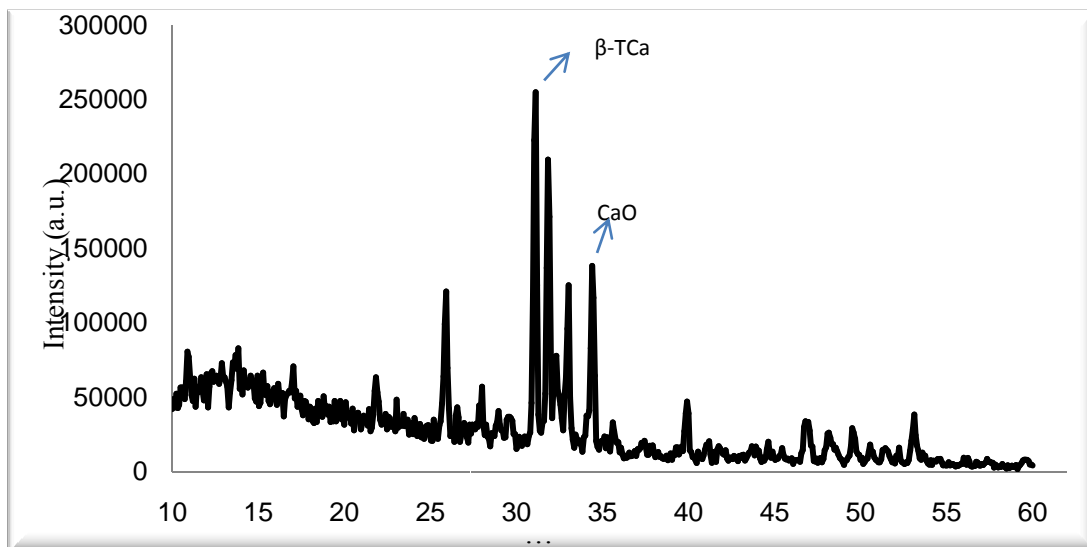
The morphology of the selected resulting powder was examined with a scanning electron microscope (HITACHI SU660 SEM) operating at 20 kV using alumina pans as sample holders. The Microstructure Measurement software was used to evaluate the crystal size. SEM was used in order to analyze the structural morphology of the samples. As can be seen

from the Fig. 2, the SEM results of hydroxyapatite samples at 700 and 950 °C reveal that the increase in temperature from 700 to 950 °C may increase average size of particles. The average size at 700 °C

was 24 nanometers with a consistent morphology while the one synthesized at 950 °C have an average size of 218 nanometers and inconsistency due to impurities.



a



B

Fig. 1 . X-ray powder diffraction pattern of nano hydroxyapatite at (a) 700⁰ C and (b) 950⁰ C.

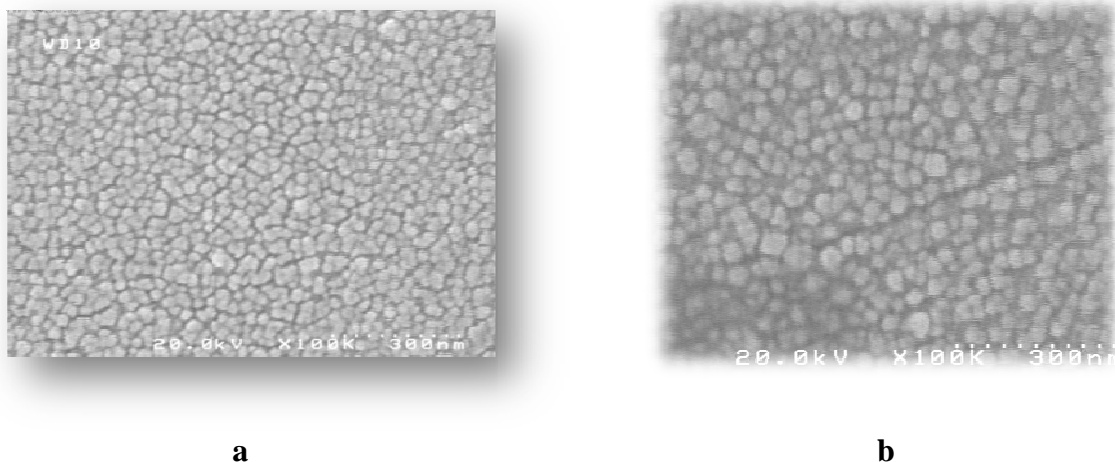


Fig. 2. SEM images of synthesized nanohydroxyapatite at (a) 700^o C and (b) 950^o C.

The effect of initial pH on adsorption capacity

It is well established that metal ion removal by both non-specific and specific sorbents is dependent on pH between 3 and 10.0 [25]. In this study, therefore, in order to establish the effect of pH on the adsorption of Hg²⁺ ions onto the nano hydroxyapatite, we repeated the batch equilibrium studies at different pH values in the range of 4– 8. Fig. 3 illustrates the effect of pH on adsorption. It is evident that the adsorption of Hg²⁺ onto the nano hydroxyapatite begins at a pH value of around 6 with the gradual linear increase up to a value of 8. The pH of the aqueous solution of Hg²⁺ affects its uptake on the nano hydroxyapatite, and the uptake increases at higher pH values. This can be explained on the basis of proton-competitive sorption reactions. One can say that at lower pH, H⁺ ions compete with Hg²⁺ ions for the surface binding sites of the adsorbent. Metal adsorption in acidic range has been described similarly by Namasivayam and Ranganathan [26], Doyurum and Celik [27], Rivastava *et al.* [28], Singh *et al.* [29], Evans *et al.* [30], Kadirvelu and Namasivayam [31], Agraval and Sahu [32], Mohan and Singh [33], and Liu *et al.* [34]. The concentration of the

hydrolyzed mercury species depends on the mercury concentration, and the solution pH. It is known that precipitation plays a major role in removing of Hg²⁺ ions in alkaline range [28]. On the other hand, the precipitation of metal hydroxides into pores or spaces around the particles is hardly possible since the sorption process is kinetically faster than the precipitation [35, 36]. Therefore, it can be said that Hg²⁺ removal onto nano hydroxyapatite was dominantly controlled by adsorption at pH values of 6.0<pH<8.0 but it could be slightly enhanced by mercury hydroxide precipitation at pH>7.0.

The effect of contact time on adsorption capacity

A 10 ml sample of metal solution with the initial concentration 200 mg/L, was added to 0.05 g of adsorbent and the concentration of Hg(II) in the solution was monitored at different times, namely 30, 60, 120, 180, 240, 300, 360, 420, 480, and 540 minutes at optimum pH, T, etc. After the reaction starts both adsorption and desorption processes occur until equilibrium is reached [37]. As Fig. 4 illustrates, the adsorption capacity of mercury increased with contact time up to 360 minutes. Afterward, there is no

considerable change in Hg(II) ion removal. Thus, one can conclude that the system attains equilibrium value at 360 minutes; this time is used for all the following equilibrium studies.

The effect of temperature on adsorption capacity

The effect of temperature on adsorption of Hg(II) ions onto hydroxyapatite nanocrystals was studied at a range of 303 to 343 K. It was found that adsorption

capacity (q_e) values increased from 318.56 to 393.42 (mg/g) as T was increased from 303 to 343 K. This slight change could be because of higher collision frequencies at higher temperature and hence leading to more sorption. A very trivial change may reflect on the saturation of surface sites by the Hg(II) ions at this range of temperatures which also leads to a thicker boundary layer between hydroxyapatite and free ions in solution [38]. The results of the experiment are shown in Fig. 5.

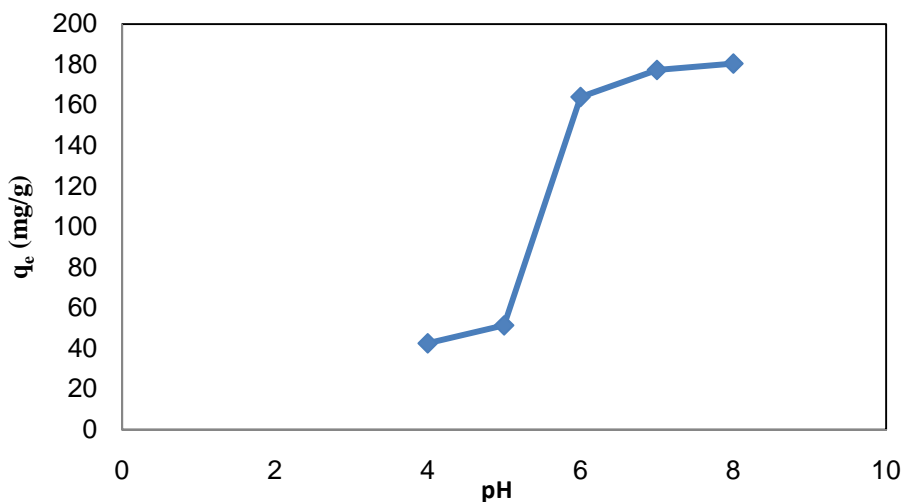


Fig. 3. Effect of pH on the Hg(II) removal onto nano hydroxyapatite.

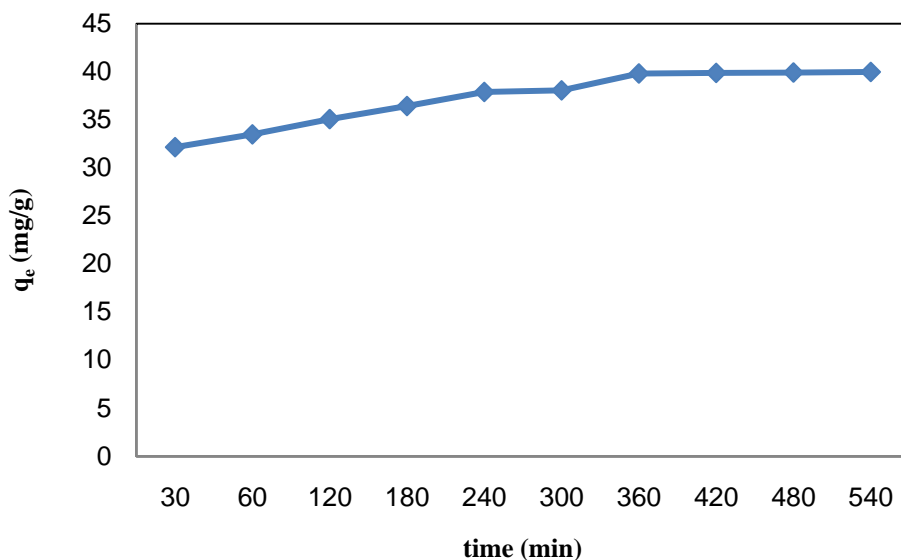


Fig. 4. Effect of time on the Hg(II) removal onto nano hydroxyapatite.

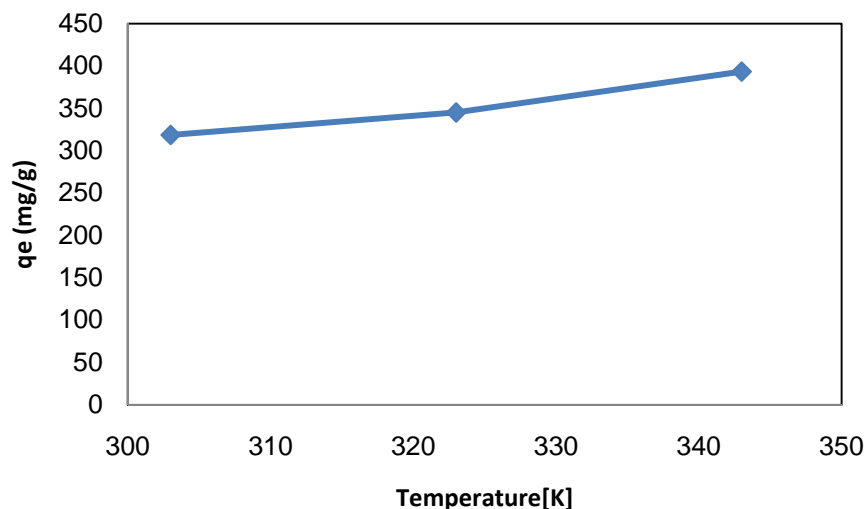


Fig. 5. Effect of temperature on the adsorption of Hg(II) on nano hydroxyapatite.

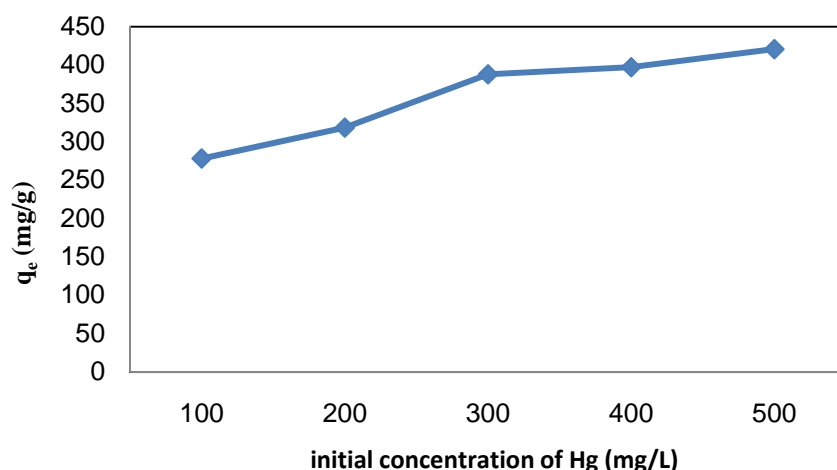


Fig. 6. Effect of initial concentration on the adsorption of Hg(II) on nano hydroxyapatite.

The effect of initial concentration on adsorption capacity

The same procedure as of the previous section was followed except for one modification: the initial concentration of Hg(II) solution was varied from 100 to 800 mg/L in increments of 100 mg/L. The amount of mercury adsorbed for varied initial concentrations onto nano hydroxyapatite was measured and the results are illustrated in Fig. 6. The removal of mercury decreased with an increase in the initial Hg(II) concentration due to lack of binding sites for the adsorption of Hg(II) ions. Yet, amount of

metal adsorbed per unit mass of adsorbent, q_e is higher at high concentrations, as shown in Fig. 6. A larger driving force for mass transfer at higher concentrations of metal ions accounts for the increase in loading capacity of the adsorbent [39]. As concentration of metal ion increases, the probability of surface adsorption increases for more ions are available per unit surface area.

Adsorption isotherm

Adsorption isotherm, at constant temperature, reveals the relation between the amount adsorbed and the equilibrium

concentration of ions in the liquid phase. Adsorption isotherm gives significant information about the mechanism of adsorption and contributes to the design of new adsorbing systems [40]. In this study, the isotherm data was analyzed using the Langmuir and Freundlich equations.

Langmuir isotherm

Langmuir isotherm models the monolayer coverage of the adsorption surface, assuming that all surface sites are energetically identical and surface itself is homogeneous. It also assumes that intermolecular forces decrease rapidly with the distance from the adsorption surface. Langmuir isotherm is expressed as:

$$q_e = \frac{K_L q_m C_e}{(1 + K_L C_e)} \quad (2)$$

The above equation can be rearranged to the following linear form:

$$\frac{C_e}{q_e} = \frac{1}{K_L q_m} + \frac{C_e}{q_m} \quad (3)$$

Values of q_m and K_L are determined from a plot of (C_e/q_e) vs. (C_e) . C_e is the equilibrium concentration of Hg(II) ion on the adsorbent (mg/L), q_e is the amount of

Hg(II) adsorbed per unit mass of nano hydroxyapatite at equilibrium concentration (mg/g), q_m (mg/g) is the maximum adsorption capacity, and K_L is Langmuir constant which is related to sorption energy; specifically, K_L shows adsorption enthalpy which generally varies with temperature [41]. The Langmuir isotherm was used for our experimental data and the results are shown in Fig. 7. A fit of the data to a single line results in a $q_m = 434.782$ mg/g and $K_L = 0.0303$ g/mg.

The Langmuir isotherm can be expressed in terms of a dimensionless constant named equilibrium parameter, R_L which is defined as:

$$R_L = \frac{1}{1 + K_L C_0} \quad (4)$$

where C_0 is the initial metal concentration. The value of R_L indicates the type of isotherm to be favorable ($0 < R_L < 1$), unfavorable ($R_L > 1$), linear ($R_L = 1$), or irreversible ($R_L = 0$) [42]. Fig. 9 shows that $0 < R_L < 0.2$ for the adsorption of Hg(II) onto nano hydroxyapatite. Since R_L is larger than zero, the adsorption process is assumed to be favorable.

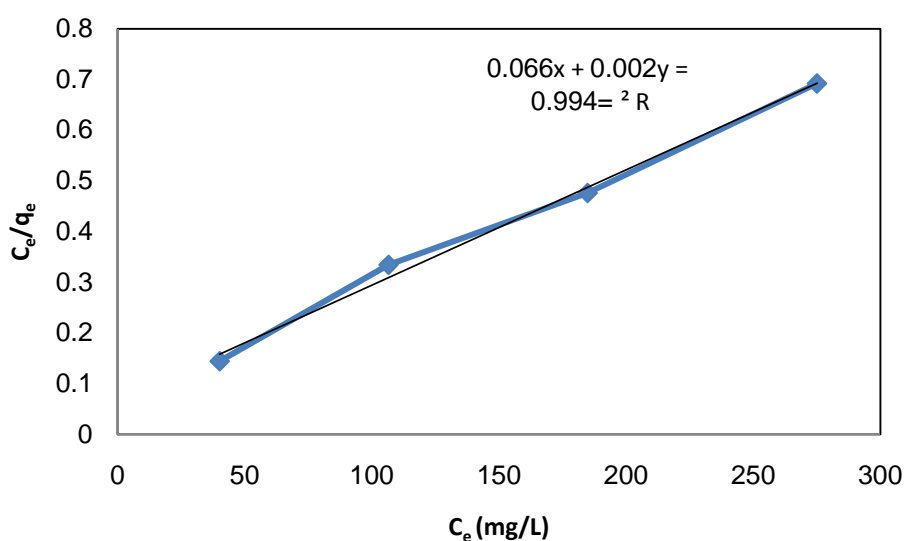


Fig. 7. Langmuir isotherm for adsorption of Hg at T = 303 K.

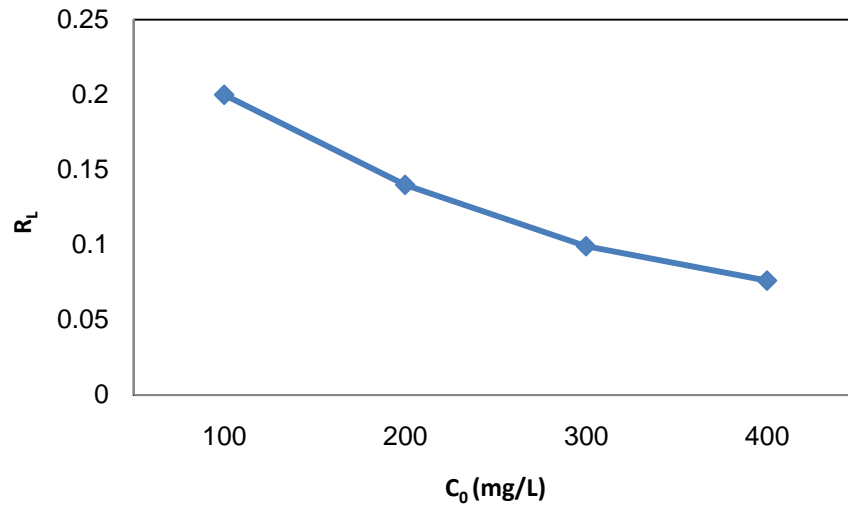


Fig. 8. Separation factor for adsorption of Hg(II) onto nano hydroxyapatite.

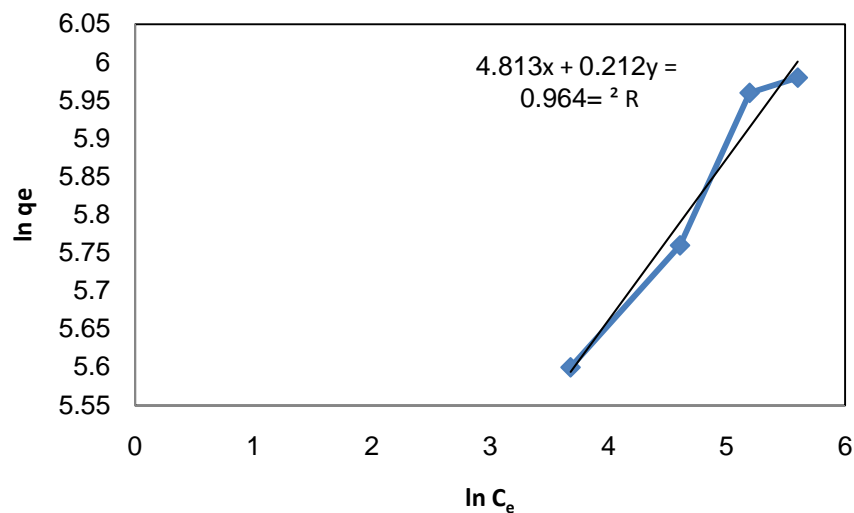


Fig. 9. Freundlich isotherm for adsorption of Hg at T = 303 K.

Freundlich isotherm

The Freundlich isotherm expresses adsorption at multilayer and on energetically heterogeneous surfaces. It is an empirical equation suitable for high and middle range of solute concentration but not for low concentrations. The Freundlich isotherm is written as [22]

$$q_e = k_F C_e^{\frac{1}{n}} \quad (5)$$

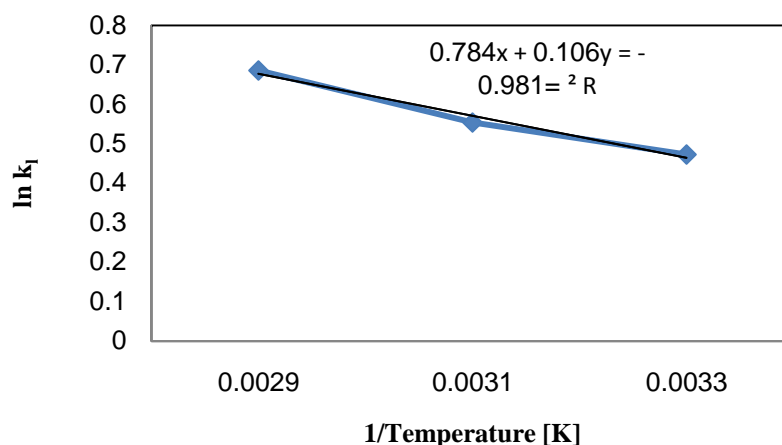
The linear form of the equation becomes,

$$\ln q_e = \ln K_F + \frac{1}{n} \ln C_e \quad (6)$$

where q_e designates the amount of mercury species adsorbed at equilibrium in mg/g, C_e is the solute equilibrium concentration in mg/L, K_F and n are Freundlich constants related to the adsorption capacity and intensity of adsorption, respectively. K_F and n were determined from plot of $\ln q_e$ vs. $\ln C_e$ as shown in Fig. 9. The calculated parameters for all of isotherms are presented in Table 1. Data from Table 1 reveals that Langmuir model acceptably fit the experimental data.

Table 1. Langmuir and Freundlich parameters for Hg(II) sorption onto nano hydroxyapatite at 303 K

	Langmuir		Freundlich
q_{\max} (mg /g)	434.7826	n	4.7170
K_L (L /mg)	0.0303	K_F (L/ g)	123.1000
R_L^2	0.9940	R_F^2	0.9640

**Fig. 10.** Plot of $\ln K_L$ versus $1/T$.**Table 2.** Thermodynamic parameters of Hg (II) adsorption onto nano hydroxyapatite

T (K)	ΔG^0 (J/mol)	ΔH^0 (J/mol)	ΔS^0 (J/mol K)
303	-1191.866		
323	-1488.942	0.88	6.5
343	-1956.617		

Determination of thermodynamic parameters

Three thermodynamic parameters: standard free energy change (ΔG^0), standard enthalpy change (ΔH^0) and standard entropy change (ΔS^0) were determined by the following equations [48].

$$K_L = \frac{q_e}{C_e} \quad (7)$$

$$\Delta G^0 = -RT \ln K_L \quad (8)$$

$$\ln K_L = \frac{\Delta S^0}{R} - \frac{\Delta H^0}{RT} \quad (9)$$

$$\Delta S^0 = \frac{\Delta H^0 - \Delta G^0}{T} \quad (10)$$

where R is the universal gas constant, 8.314 J/mol K; T is the absolute

temperature (K), and K_L is the Langmuir constant (mol/L). The thermodynamic parameters of adsorption have been studied at a range of 303 to 343 K. Fig. 10 shows a plot of $\ln K_L$ versus $1/T$ fitted to a straight line (Eq. (9)); ΔH^0 and ΔS^0 values were calculated from the slope and intercept, respectively, as shown in Table 2. ΔG values for the adsorption of Hg (II) onto nano hydroxyapatite ranges from -1.19 to -1.95 kJ/mol, suggesting a physical adsorption process enhanced by electrostatic effect. The negative sign of ΔG expresses spontaneous nature of the reaction whereas positive values of ΔG confirm its endothermicity. The positive value of ΔS shows an overall entropy increase.

CONCLUSIONS

The synthesis of nanocrystalline hydroxyapatite powder via sol-gel combustion method was prepared and characterized using XRD and SEM analysis. The adsorption strongly depends on the parameters such as initial concentration of Hg(II), pH, contact time, and temperature. The data revealed that the solution pH is a key factor affecting the

adsorption characteristics. The adsorption process follows Langmuir isotherm which fits well heterogeneous surfaces. Adsorption of Hg(II) ions onto nano hydroxyapatite obeyed at pH 7.0. It was concluded from the values of the thermodynamic parameters that the adsorption process is spontaneous and endothermic in nature.

REFERENCES

- [1] H. D. Doan, J.Wu, R. Mitzakov, J. Chem. Technol. Biotechnol. 81 (2006) 1398–1408.
- [2] O. J. Esalah, M.E. Weber, J.H. Vera, Can. J. Chem. Eng. 78 (2000) 948–954.
- [3] A. I. Zouboulis, K.A. Matis, B.G. Lanara, C. Loos-Neskovic, Sep. Sci. Technol. 32 (1997) 1755–1767.
- [4] C. A. Toles, W.E. Marshall, Sep. Sci. Technol. 37 (2002) 2369–2383.
- [5] V. Ravindran, M.R. Stevens, B.N. Badriyha, M. Pirbazari, AIChE J. 45 (1999) 1135–1146.
- [6] L. Canet, M. Ilpide, P. Seta, A. Sep. Sci. Technol. 37 (2002) 1851–1860.
- [7] P. Miretzky, A. Saralegui, A.F. Cirelli, Chemosphere 62(2006) 247–254.
- [8] S. Schiewer, B. Volesky, Environ. Sci. Technol. 29(1995) 3029–3058.
- [9] Krestou, A. Xenidis, D. Pnias, tuff. Miner. Eng. 16 (2004) 1363–1370.
- [10] M. Czerniczyniec, S. Farias, J. Magallanes, D. Cicerone, 11th International Conference on Surface and Colloid Science, Foz do Iguazu, Brazil, pp. (2003) 269.
- [11] E. D. Vega, J.C. Pedregosa, G.E. Narda, J. Phys. Chem. Solids 60 (1999) 759–766.
- [12] J. Reichert, J. Binner, J. Mater. Sci. 31(1996) 1231–1241.
- [13] Leyva, J. Marrero, P. Smichowski, D. Cicerone, Environ. Sci. Technol. 35 (2001) 3669–3675.
- [14] Fuller, J. Bargar, J. Davis, M. Piana, Environ. Sci. Technol. 36(2002) 158–165.
- [15] S. McGrellis, J. Serafini, J. Jean, J. Pastol, M. Fedoroff, Sep. Purif. Technol. 24 (2001) 129–138.
- [16] X. Chen, J.V. Wright, J.L. Conca, L. M. Peurrung, Environ. Sci. Technol. 31 (1997) 624–631.
- [17] V. Laperche, S.J. Traina, P. Gaddam, T.J. Logan, J.A. Ryan, Environ. Sci. Technol. 30 (1996) 3321–3326.
- [18] Q.Y. Ma, S.J. Traina, T.J. Logan, J.A. Ryan, Environ. Sci. Technol. 27 (1993) 1803–1810.
- [19] Q.Y. Ma, S.J. Traina, T.J. Logan, J.A. Ryan, Environ. Sci. Technol. 28 (1994) 1219–1228.
- [20] E. Mavropoulos, A.M. Rossi, A.M. Costa, C.A. Perez, J.C. Moreira, M. Saldanha, Environ. Sci. Technol. 36 (2002) 1625–1629.
- [21] Nzihou, P. Sharrock, Waste Manage. 2002 (2002) 235–239.
- [22] Y. Takeuchi, H. Arai, J. Chem. Eng. Jpn. 23 (1990) 75–80.
- [23] J. C. Elliott, Elsevier, Amsterdam (1994).
- [24] H. Tanaka, M. Futaoka, R. Hino, K. Kandori, T. Ishikawa, J. Colloid Interface Sci. 283 (2005) 609–612.
- [25] C. Arpa, R. Say, N. Satiroglu, S. Bektas, Y. Yurum, O. Genc, Turk. J. Chem. 24 (2000) 209.

- [26] C. Namasivayam, K. Ranganathan, *Environ. Technol.* 16 (1995) 851.
- [27] S. Doyurum, A. Celik, *J. Hazard. Mater. B* 138 (2006) 22.
- [28] V. C. Srivastava, I.D. Mall, I.M. Mishra, *Chem. Eng. J.* 117 (2006) 79.
- [29] D. B. Singh, D.C. Rupainwar, G. Prasad, K.C. Jayaprakas, *J. Hazard. Mater.* 60 (1998) 29.
- [30] J. R. Evans, W.G. Davids, J.D. MacRae, A. Amirbahman, *Water Res.* 36 (2002) 3219.
- [31] K. Kadirvelu, C. Namasivayam, *Adv. Environ. Res.* 7 (2003) 471.
- [32] Agrawal, K. K. Sahu, *J. Hazard. Mater. B*137 (2006) 915.
- [33] D. Mohan, K.P. Singh, *Water Res.* 36 (2002) 2304.
- [34] Y. Liu, X. Chang, Y. Guo, S. Meng, *J. Hazard. Mater. B* 135 (2006) 389.
- [35] R. L. Ramos, J.R.R. Mendez, J.M. Baron, L. F. Rubio, R. M. G. Coronado, *Water Sci. Technol.* 35 (1997) 205.
- [36] B. M. Babic, S.K. Milonjic, M.J. Polovina, S. Cupic, B.V. Kaludjerovic, *Carbon* 40 (2002) 1109.
- [37] W. S. W. Ngah, S. Fatinathan J. *Environ. Manag.* 91 (2010) 958–969.
- [38] L. Bulgariu, M. Ratoi, D. Bulgariu, M. Macoveanu, *Environ. Eng. Manag. J.* 7 (2008) 511–516.
- [39] N. Unlü, M. Ersoz, *J. Hazard. Mater.* 136 (2006) 272–280.
- [40] A. H. Mahvi, A. Maleki, A. Eslami, *Am. J. Appl. Sci.* 1 (2004) 321–326.
- [41] E. Erdem, N. Karpinar, R. Donat, *J. Coll. Interface Sci.* 280 (2004) 309–314.
- [42] W. S. W. Ngah, A. Kamari, Y.J. Koay, *Int. J. Biol. Macromol.* 34 (2004) 155–161.
- [43] K. H. Chong, B. Volesky, *Biotech. Bioeng.* 47 (1995) 451–460.